



Consequences of variations in spatial turbulence characteristics for fatigue life time of wind turbines

Larsen, Gunner Chr.

Publication date:
1998

Document Version
Publisher's PDF, also known as Version of record

[Link back to DTU Orbit](#)

Citation (APA):
Larsen, G. C. (1998). *Consequences of variations in spatial turbulence characteristics for fatigue life time of wind turbines*. Denmark. Forskningscenter Risoe. Risoe-R No. 1052(EN)

General rights

Copyright and moral rights for the publications made accessible in the public portal are retained by the authors and/or other copyright owners and it is a condition of accessing publications that users recognise and abide by the legal requirements associated with these rights.

- Users may download and print one copy of any publication from the public portal for the purpose of private study or research.
- You may not further distribute the material or use it for any profit-making activity or commercial gain
- You may freely distribute the URL identifying the publication in the public portal

If you believe that this document breaches copyright please contact us providing details, and we will remove access to the work immediately and investigate your claim.

Consequences of Variations in Spatial Turbulence Characteristics for Fatigue Life Time of Wind Turbines

Gunner Chr. Larsen

DISTRIBUTION OF THIS DOCUMENT IS UNLIMITED
FOREIGN SALES PROHIBITED

DISCLAIMER

Portions of this document may be illegible in electronic image products. Images are produced from the best available original document.

Consequences of Variations in Spatial Turbulence Characteristics for Fatigue Life Time of Wind Turbines

Gunner Chr. Larsen

Abstract

The turbulence level and the spatial structure of the turbulence, at a particular site, depend on the topography of the terrain. The fatigue loading of a turbine is strongly related to the turbulence conditions, and thereby also to the topography of the site. Consequently, the fatigue loading in complex terrain might differ significantly from fatigue loading in flat and homogeneous terrain.


The turbulence level is known to play a key role in the fatigue loading of vital wind turbine components. However, also the spatial turbulence structure might be of significance in relation to fatigue loading. In the present analyses, the fatigue loading of wind turbines, situated in complex terrain, is investigated in order to determine the crucial parameters, in a traditional description of the spatial structure of the turbulence, in such situations. The parameter study is performed by means of numerical calculations, and it embraces three different wind turbine types, representing a pitch controlled concept, a stall controlled concept, and a stall controlled concept equipped with an extremely flexible tower.

For each of the turbine concepts, the fatigue load sensibility to the selected turbulence characteristics are investigated for three different mean wind speeds at hub height. The selected mean wind speeds represent the linear-, the stall-, and the post stall aerodynamic region for the stall controlled turbines and analogously the unregulated-, the partly regulated-, and the fully regulated regime for the pitch controlled turbine. Denoting the turbulence component in the mean wind direction by u , the lateral turbulence component by v , and the vertical turbulence component by w , the selected turbulence characteristics comprise the u -turbulence length scale, the ratio between the v - and w -turbulence intensities and the u -turbulence intensity, the uu -coherence decay factor, and finally the u - v and u - w cross-correlations.


The overall conclusion is that the selected variation of the u -turbulence length scale has a significant effect on the fatigue loads, that the effects of variations of the relative v - and w -turbulence intensities are moderate, that also the modification in the uu -coherence decay factor has a moderate effect, and, finally, that the investigated u - v and u - w cross-correlations are without importance. In general, the parameter sensitivities are increased considerably if the stall controlled turbine, instead of the conventional tower, is equipped with a very flexible tower.

The work reported makes part of the project "Investigation of Design Aspects & Design Options for Wind Turbines Operating in Complex Terrain Environments" (COMTERID), which is co-funded through JOULEIII on contract no. JOR3-CT95-0033.

The present report has passed an internal review at the Wind Energy and Atmospheric Physics Department, Risø, performed by:



Søren M. Petersen



Per Vølund

ISBN 87-550-2432-7
ISBN 87-550-2433-5 (Internet)

ISSN 0106-2840

Information Service Department, Risø, 1998

Contents

1 INTRODUCTION	5
2 NUMERICAL PROCEDURE	6
2.1 Aeroelastic models	6
2.2 Fatigue evaluation	7
2.3 Simulation matrix	8
3 RESULTS	10
3.1 NTK500 equipped with stiff tower	10
3.2 NTK500 equipped with soft tower	13
3.3 Vestas V39	16
4 CONCLUSION	19
5 REFERENCES	20
APPENDIX A	21
APPENDIX B	28

1 Introduction

During recent years, a huge potential for installation of wind turbines in complex mountainous terrain has been recognised due to favourable wind resources covering large areas, which are not extensively utilised.

The design calculations for a turbine depend strongly on the turbulence conditions, which are the main responsible for the fatigue loading of vital wind turbine components. The turbulence characteristics at a particular site are known to depend strongly on the wind inflow conditions and thereby on the topography of the terrain. Consequently, the turbulence characteristics associated with a complex terrain site differ from that associated with a flat terrain site.

The dominating turbulence parameter, regarding fatigue loading of turbines, is the turbulence intensity associated with the mean wind direction (Morfiadakis, 1996). In addition to that, the spatial structure of the turbulence is of relevance. The purpose of the present study is to investigate which of the parameters, in a traditional parameterization of the spatial structure of the turbulence, that is of particular importance regarding the fatigue loading of turbines situated in complex terrain. This type of parameter investigation is hard to perform through experiments, and consequently a numerical procedure is selected.

Three different wind turbine types are selected for the analysis, representing a pitch controlled concept, a stall controlled concept, and a stall controlled concept with an extremely flexible tower. All the involved turbine concepts are traditional three bladed, upwind and constant speed machines with an active yaw mechanism. For each of the turbine concepts, the fatigue load sensibility to the selected turbulence characteristics are investigated for three different mean wind speeds at hub height. The selected mean wind speeds represent the linear-, the stall-, and the post stall aerodynamic region for the stall controlled turbines and analogously the unregulated-, the partly regulated-, and the fully regulated regime for the pitch controlled turbine.

The report is structured as follows. Chapter 2 contains a brief description of the aeroelastic modelling of the selected turbine concepts, the fatigue evaluation procedure, and of the load cases defining the parameter study. In Chapter 3, the results from the investigation are presented, and finally the conclusions are drawn in Chapter 4.

2 Numerical Procedure

The type of parameter investigation intended for the present analysis is hard to perform through experiments, and consequently a numerical procedure is selected. The numerical procedure involves a number of distinct but related steps - establishment of aeroelastic models of the selected turbines, definition and simulation of the relevant load cases, and finally a fatigue analysis of the predicted structural loads.

2.1 Aeroelastic models

The response calculations performed in the present analysis are based on the aeroelastic code HawC, and on the turbulence generator code SOSISC.

HawC (Thirstrup Petersen, 1990), is basically a finite element model developed as a special purpose wind turbine model. The structural part of the model is based on 2-node prismatic beam elements with 6 degrees of freedom at each node, corresponding to 3 translations and 3 rotations. The aerodynamic loads are derived by use of a quasi-steady theory, based on combined blade element- and momentum theory.

The SOSISC turbulence generator (Carlén) is a newly developed turbulence generator, which is capable of taking arbitrary specified correlations between the three cartesian turbulence components into account. The model assumes that the turbulence is homogeneous in space.

Three different wind turbine types are modelled, representing a pitch controlled concept, a stall controlled concept, and a stall controlled concept equipped with an extremely flexible tower. All the involved turbine concepts are traditional three bladed, upwind and constant speed machines with an active yaw mechanism.

The selected conventional stall controlled turbine is the Nordtank 500/37 turbine, and the associated aeroelastic model is verified in (Vøglund, 1997). The stall controlled concept equipped with the extremely flexible tower is basically identical to the Nordtank 500/37 model, except that the tower is softened drastically such that the first tower bending frequency is changed from being well above the 1P frequency to below this frequency. The specific change in the tower frequency is illustrated in Figure 2.1-1, where it appears that the tower frequency is shifted from 0.83 Hz to 0.27 Hz. The 1P rotational frequency is equal to 0.5 Hz. The soft tower is derived from the conventional tower simply by reducing all cross sectional moments of inertia with a suitable (constant) factor. It should be stressed, that this simple procedure is likely to result in a turbine structure which is not dynamically optimised, and this might in turn affect the generality of the results obtained for the soft tower design. However, results from a more comprehensive study (Larsen, 1998) indicates that there is no significant influence from unfavourable resonances in the present results.

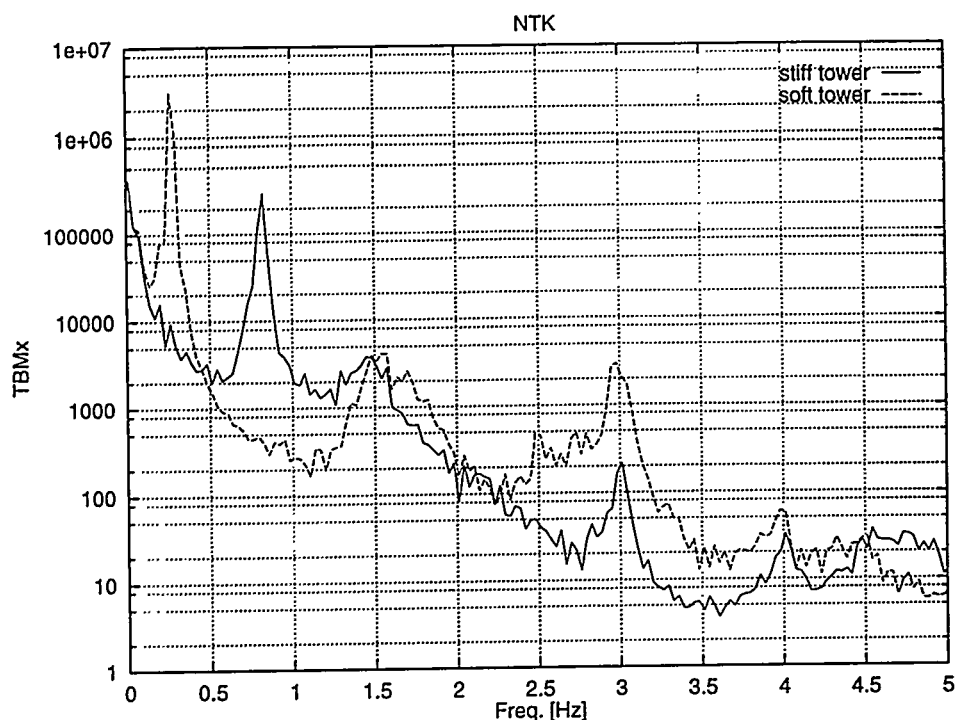


Figure 2.1-1 Power spectrum of tower bottom moment showing the first tower bending frequency of Nordtank 500/37 equipped with conventional- and soft tower, respectively.

The selected conventional pitch regulated turbine is the Vestas V39 turbine, and the associated aeroelastic model is verified in (Larsen, 1998).

2.2 Fatigue evaluation

Based on the results produced by the performed aeroelastic time simulations, the Rainflow Counting Procedure is used to determine the involved load cycles for each of the selected load signals. The Rainflow Counting Procedure synthesise local maxima and minima to load range cycles, interpreted as closed hysteresis curves in the load history of the particular material. In the present situation 50 levels were used to resolve the load range interval.

Having evaluated the Rainflow Spectrum, the fatigue effects, of the associated spectral components, are subsequently decoupled applying the Palmgren-Miner approach to concentrate the spectral information in only one number, expressing the corresponding fatigue damage. In the present analysis, the fatigue damage estimation has been based on Wöhler exponent 12 for blade loads and on 4 for the remaining structural loads. The results are presented in terms of equivalent moments giving identical fatigue damage with reference to a 1 Hz cycle frequency.

Usually, more than one (typically between 3 and 6) 10-minutes load time series are required in order to make fatigue estimates converge to a reasonable level. This is primarily due to the demand for sufficient statistical significance of the low-frequency turbulence contribution to the fatigue life consumption. However, as the post-processing involves only the relative difference between fatigue load estimates referring to the same turbulence field, a single representation of each load case was considered sufficient.

2.3 Simulation matrix

To approach a complex terrain situation as close as possible, three reference load situations are selected based on an extensive measurement campaign conducted at Agia Marina in Greece.

As previously mentioned, the scope of the parameter analysis is the connection between the spatial structure of the 3D turbulence and the fatigue loading of turbines. In accordance with the traditional turbulence parameterization, the turbulence intensity, the turbulence length scale, and coherence decay factors are selected as relevant parameters for the investigation.

The three selected reference load situations refer to hub mean wind speeds representing the linear-, the stall-, and the post stall aerodynamic region (10 m/s, 14 m/s, and 18 m/s, respectively). For each of these, suitable variations in the turbulence parameters are selected based on the Agia Marina experimental data base. In order to simplify the analysis, only parameter variations, a priori considered of primary importance for fatigue, are considered.

Denoting the turbulence component in the mean wind direction by u , the lateral turbulence component by v , and the vertical turbulence component by w , the primary turbulence parameters are considered to be the ratio between the v - and w -turbulence intensities and the u -turbulence intensity (equal to 15%), the u -turbulence length scale, the uu -coherence decay factor, and finally the u - v and u - w cross-correlations (the v - w cross-correlation turned out to be neglectable compared to the remaining correlations). For each of these, mean values extracted from the experimental data base define the reference states (together with mean values of the turbulence parameters of only secondary importance). The selected variation is defined as the one standard deviation of the respective parameter.

In general, the autocorrelation of a stationary random process is an even function, whereas the cross-correlation function of two stationary processes is the sum of an even and an odd function. Consequently, the Fourier transform of an autocorrelation function is a real function, whereas the Fourier transform of a cross-correlation function (in general) is a complex function. In a first order approach it was decided to simplify the analysis by neglecting the imaginary part of the Fourier representation of the u - w cross-correlation and the real part of the Fourier representation of the u - v cross-correlation.

A somewhat heuristic interpretation of the above assumptions is the following. Negligence of the imaginary part of the Fourier representation of the u - w cross-correlation implies that, in a statistical sense, there will be no phase lag between the u - and w turbulence components. Depending on the sign of the real part of Fourier representation of the u - w cross-correlation, the two velocity components will (in a statistical sense) be either negatively correlated or positively correlated, with the degree of correlation determined by the magnitude of the coherence. Now, in the atmospheric boundary layer, the u - w Reynolds stress is known to be negative, whereby, in a statistical sense, an increasing u -component will be associated with a decrease in the w -component, thus forming eddy like turbulence structures in the u - w plane. Concerning the u - v plane, the situation is as follows. Negligence of the real part of the Fourier representation of the u - v correlation implies that, in a statistical sense, there will be a phase lag equal to 90 degrees between the u - and v turbulence components. For a given point in space and for a given frequency, a “sinus” varying u -component will be accompanied by a “sinus” varying v -component, displaced with a phase lag of 90 degrees relative to the u component, thus forming patches composed of half circle arcs in the horizontal u - v plane (for coherence equal to one). For the situation with a coherence less than one, the structure of the “path” in the u - v plane will be similar, but the half circles will be less pronounced. Now, if incompressibility is assumed, the above sketched picture for a point displaced in space will be reversed concerning the sign of the v turbulence component, and hourglass like structures in the v - u plane will consequently be formed by the horizontal turbulence flow.

Beside the above simplifications, it was decided to neglect influence from mean wind shear.

For each of the mean wind speed regimes, the resulting simulation matrix appears from Table 2.3-1, where all dimensional quantities are given in S.I. units, σ denotes standard deviation, L von Karman turbulence length scale, A is a coherence decay factor, and subscripts indicate relevant turbulence components. For each mean wind speed category, the standard deviation of the longitudinal turbulence component, σ_u , is kept constant, corresponding to a u-turbulence intensity equal to 15%. The applied spectral formulation is elaborated in Appendix B.

Case	σ_v/σ_u	σ_w/σ_u	L_u	L_v	L_w	A_{uu}	A_{vv}	A_{ww}	u-w corr.	u-v corr.
1	0.85	0.66	60	30	15	5	5	5	active	active
2	1.00	0.66	60	30	15	5	5	5	active	active
3	0.85	0.76	60	30	15	5	5	5	active	active
4	0.85	0.66	30	30	15	5	5	5	active	active
5	0.85	0.66	60	30	15	7	5	5	active	active
6	0.85	0.66	60	30	15	5	5	5	non-active	non-active

Table 2.3-1 Simulation matrix used for the three mean wind regimes.

Within the assumed approximations, the u-w and u-v cross-coherences are defined by

$$Coh_{uw}(\omega) = \frac{\sqrt{\text{Re}[\mathcal{F}\{R_{uw}\}]^2 + \text{Im}[\mathcal{F}\{R_{uw}\}]^2}}{\sqrt{\mathcal{F}\{R_{uu}\}\mathcal{F}\{R_{ww}\}}} = \frac{\text{Re}[\mathcal{F}\{R_{uw}\}]}{\sqrt{\mathcal{F}\{R_{uu}\}\mathcal{F}\{R_{ww}\}}}, \text{ and}$$

$$Coh_{uv}(\omega) = \frac{\sqrt{\text{Re}[\mathcal{F}\{R_{uv}\}]^2 + \text{Im}[\mathcal{F}\{R_{uv}\}]^2}}{\sqrt{\mathcal{F}\{R_{uu}\}\mathcal{F}\{R_{vv}\}}} = \frac{\text{Im}[\mathcal{F}\{R_{uv}\}]}{\sqrt{\mathcal{F}\{R_{uu}\}\mathcal{F}\{R_{vv}\}}},$$

where R denotes a covariance function, \mathcal{F} symbolises the Fourier transform operator, and ω is the frequency. $\text{Re}[\]$ and $\text{Im}[\]$ denote the real- and the imaginary part of a complex quantity, respectively.

The u-w and u-v coherences are assumed to be on the form

$$Coh_{ij}(\omega) = B_{ij} \exp(-A_{ij}\omega), \quad (\text{no summation})$$

where i and j refer to either u , v , or w . The relevant constants A and B , defining the (active) u-w and u-v cross-correlations, are derived from data fitting in the Agia Marina data base. The following representative values have thus been obtained.

A_{uw}	A_{uv}	B_{uw}	B_{uv}
11.85	16.6	-0.55	0.2

Table 2.3-2 Constants defining the u-w and the u-v correlations.

In case the u-w and u-v cross-correlations are not active, the respective A and B constants reduce to zero.

3 Results

For each wind turbine concept and for each of the defined load situations, the equivalent moments, for a number of selected structural quantities, are determined along the lines described in section 2.2. The selected structural responses embrace the flap wise blade root moment (RFM), the edge wise blade root moment (REM), the tower bottom bending moment normal to the mean wind direction (TBMx), the tower bottom bending moment parallel to the mean wind direction (TBMy), the tower top torsion moment (TTM), the drive train (low speed) shaft torque (DTM), and a shaft bending moment (DTMz).

In the following, the conventional stall controlled turbine is denoted NTK500; STIFF, the stall controlled turbine equipped with the extremely flexible tower is indicated by NTK500; SOFT, and the pitch controlled turbine is named V39. All the results have been normalised with respect to load case 1 (see Table 2.3-1), and the relative importance of the performed parameter variations appears from the figures in the following sections. If some symbols seemingly are missing, it is due to merging of several symbols in the typography.

3.1 NTK500 equipped with stiff tower

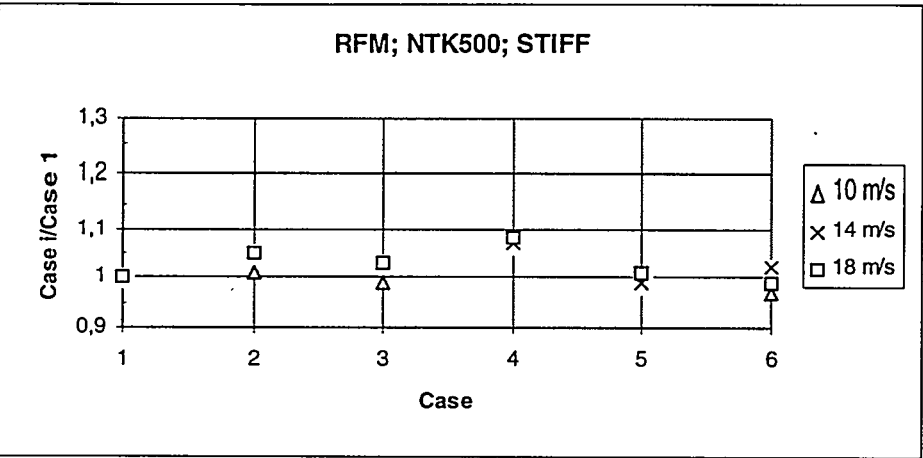


Figure 3.1-1 Relative importance of the selected parameter variations on RFM.

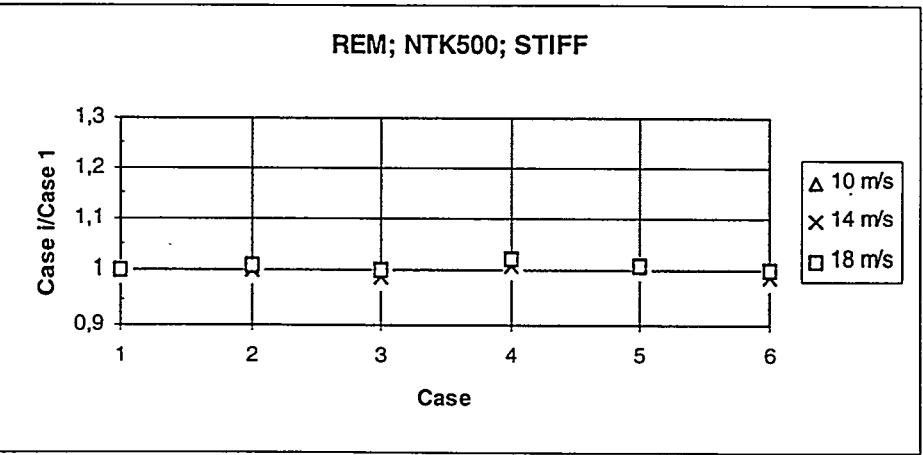


Figure 3.1-2 Relative importance of the selected parameter variations on REM.

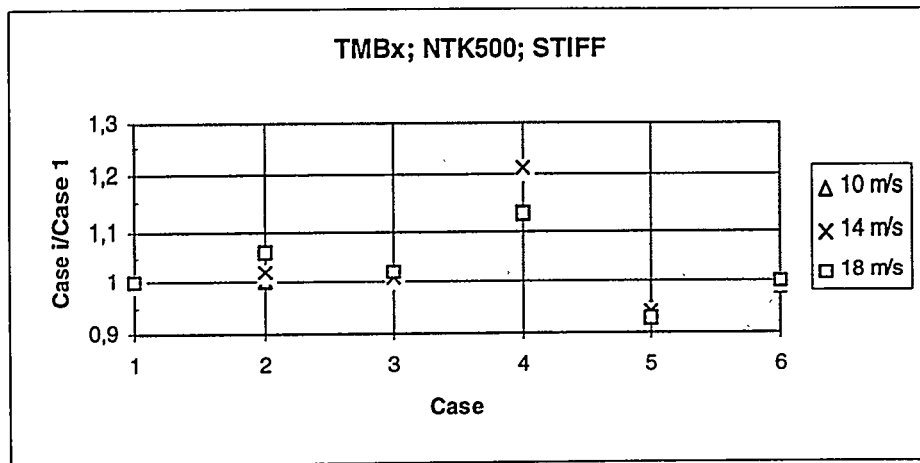


Figure 3.1-3 Relative importance of the selected parameter variations on TBMx.

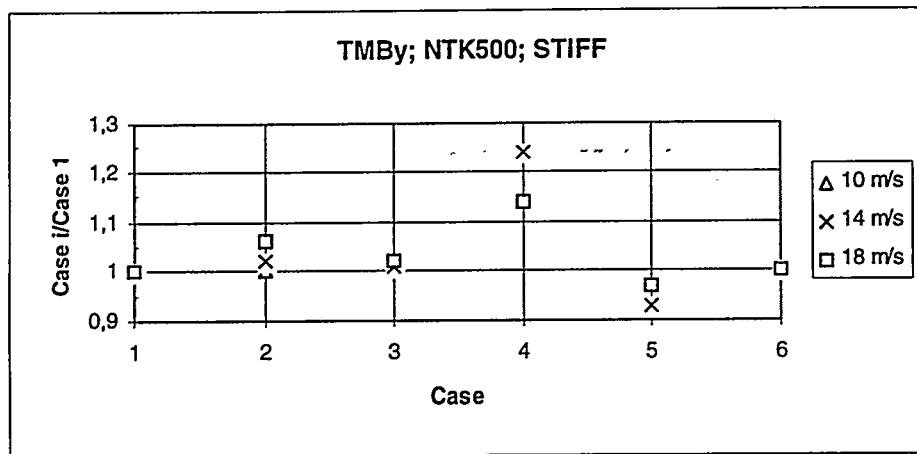


Figure 3.1-4 Relative importance of the selected parameter variations on TBM_y.

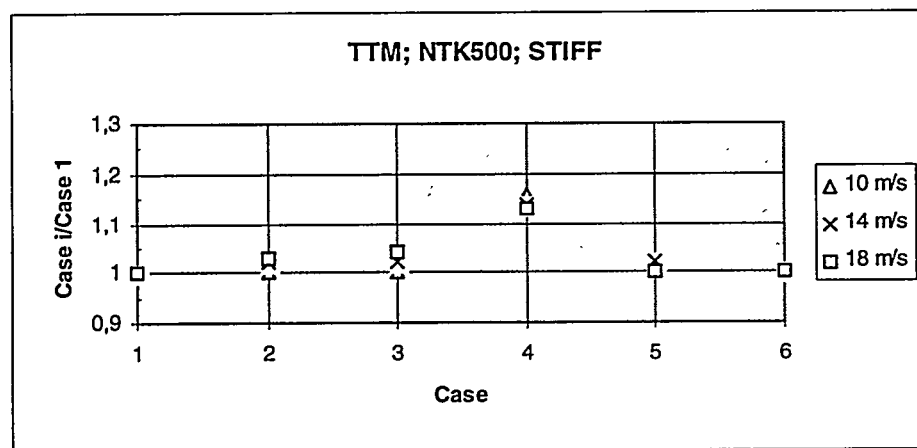


Figure 3.1-5 Relative importance of the selected parameter variations on TTM.

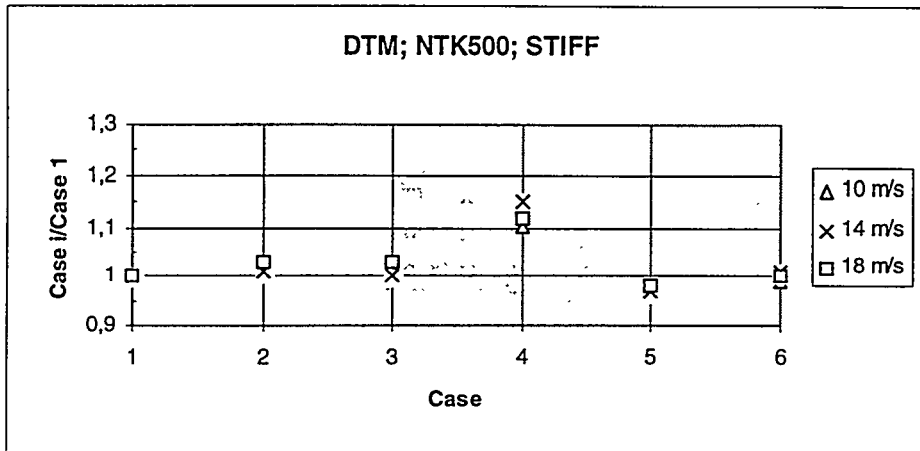


Figure 3.1-6 Relative importance of the selected parameter variations on DTM.

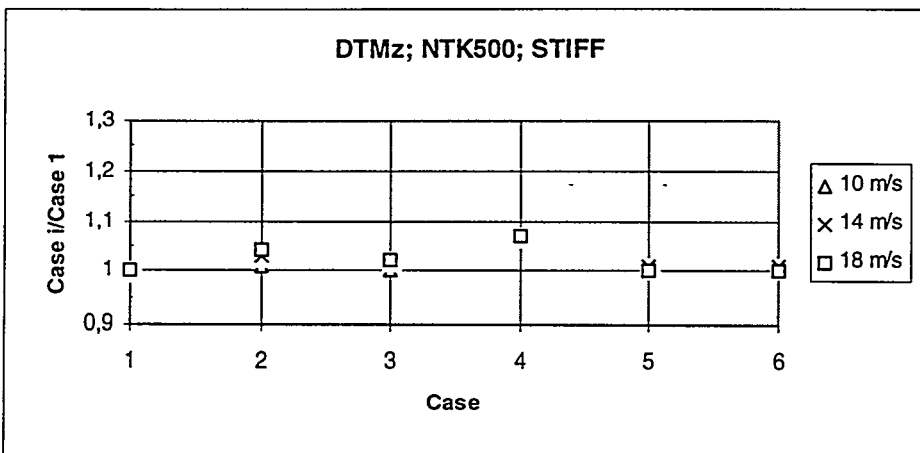


Figure 3.1-7 Relative importance of the selected parameter variations on DTMz.

The results are evaluated according to the rather arbitrary criteria that a significant relative change in equivalent moment, caused by a parameter variation, must be at least 5 %.

From Figure 3.1-1 to Figure 3.1-7 the following observations can thus be extracted:

- None of the investigated parameter variations affect the root edge wise equivalent moment significantly.
- The variation of L_u (case 4) has by far the most pronounced load consequences. The tower loading is increased with 15 % to 25 % (most severe in the stall region), the drive train loading with 10 % to 15 %, and the flap loads of the order of magnitude 5 %. The dependence of the load increase with the mean wind speed is most pronounced for the tower bottom bending moments and for the drive train torque.
- The variation of σ_v/σ_u (case 2) affects only significantly the flap load and the tower bottom bending loading in the post stall wind regime.
- The variation of σ_w/σ_u (case 3) does not give rise to any significant fatigue load consequences.
- The variation of A_{uu} (case 5) causes the tower bottom equivalent moments to be decreased of the order of magnitude 8 % - the remaining structural loads are only insignificantly affected. This include the rotor moment(s), and consequently the reduction in tower bottom loading is primary due to a reduction in the thrust forcing.
- The inclusion of the specified u-w and u-v turbulence cross-correlations is without importance for the investigated fatigue loads.

3.2 NTK500 equipped with soft tower

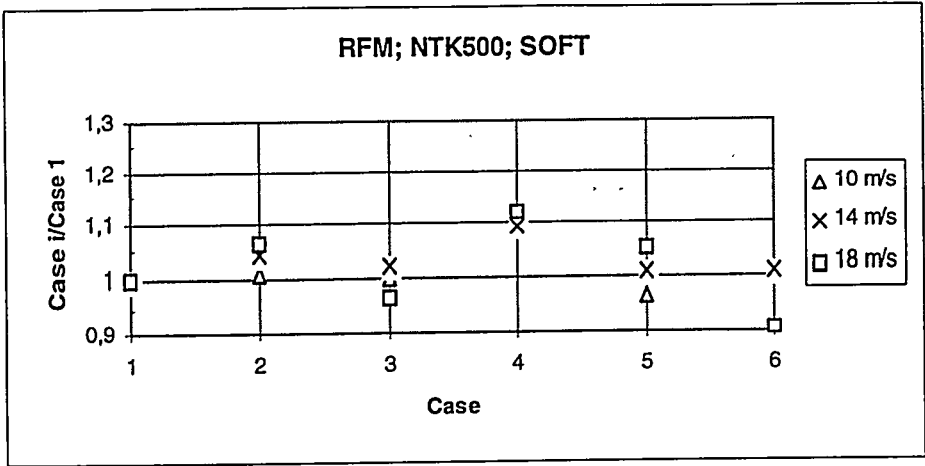


Figure 3.2-1 Relative importance of the selected parameter variations on RFM.

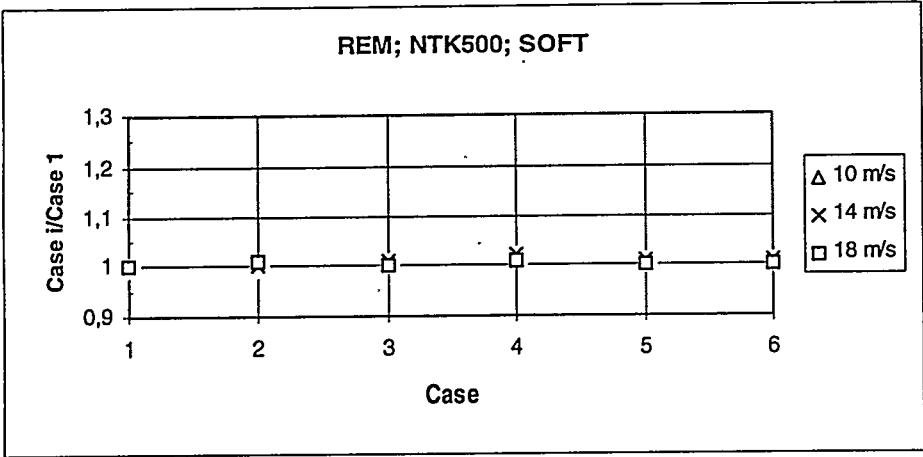


Figure 3.2-2 Relative importance of the selected parameter variations on REM.

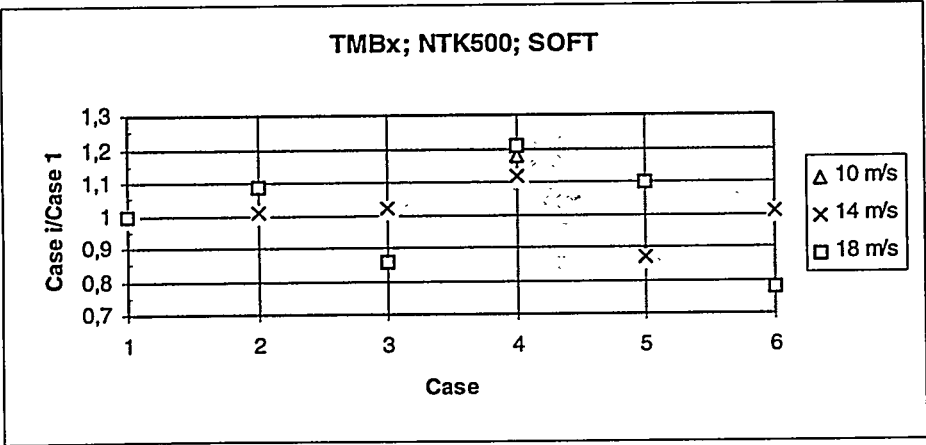


Figure 3.2-3 Relative importance of the selected parameter variations on TMBx.

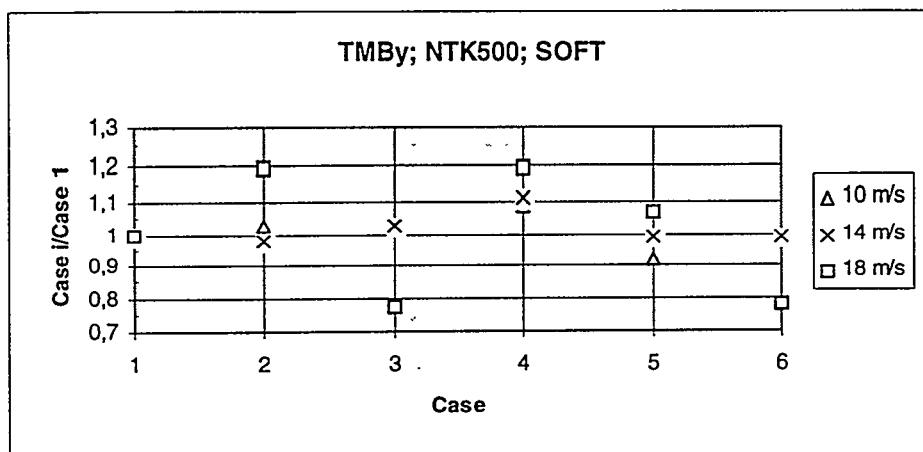


Figure 3.2-4 Relative importance of the selected parameter variations on TMBY.

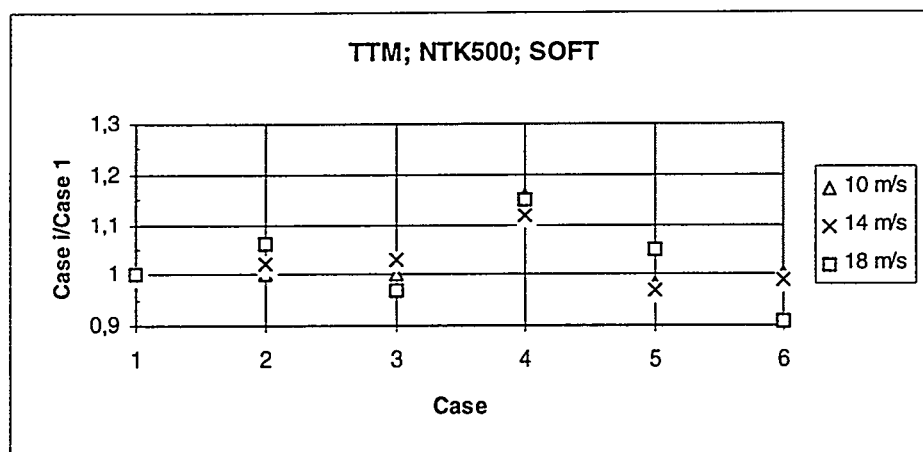


Figure 3.2-5 Relative importance of the selected parameter variations on TTM.

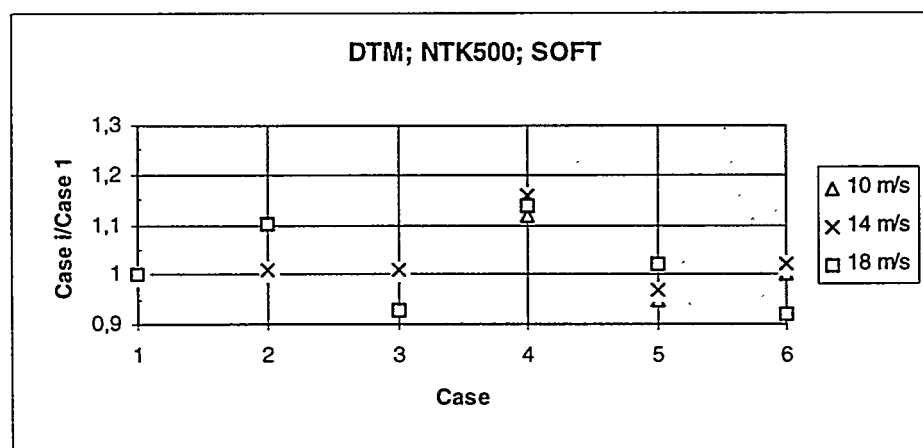


Figure 3.2-6 Relative importance of the selected parameter variations on DTM.

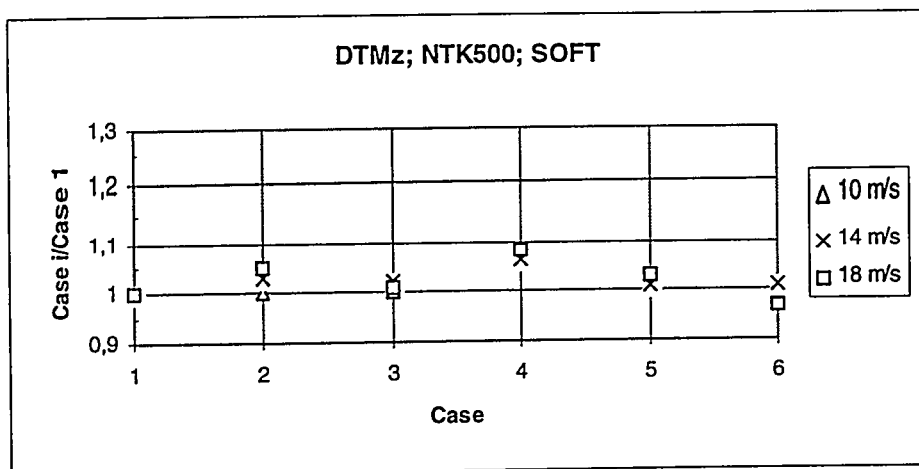


Figure 3.2-7 Relative importance of the selected parameter variations on DTMz.

From Figure 3.2-1 to Figure 3.2-7 the following observations are extracted:

- Generally, the NTK500 turbine equipped with the “soft” tower is much more sensitive to the performed parameter variations than the NTK500 turbine equipped with the conventional tower considered in section 3.1. Apart from the edge wise equivalent moment, all the parameter variations give rise to significant changes in most of the investigated fatigue loads. For some of the parameters, qualitative differences are observed for different mean wind regimes - for some mean wind speeds, a parameter variation thus results in increased fatigue loading, while at other mean wind speeds the same parameter variation results in decreased fatigue loading.
- The variation of σ_w/σ_u (case 2) affects significantly all the investigated categories of fatigue loading except the edge wise blade loading. Especially for the tower bottom bending loading, a considerable variation with the mean wind speed is observed.
- The variation of σ_w/σ_u (case 3) affects significantly the tower bottom moments and the drive train torque with the most pronounced effects at high mean wind speeds.
- The variation of L_u (case 4) influences significantly all the investigated categories of fatigue loading except the edge wise blade loading. The variability of the investigated parameter effects with the mean wind speed is moderate. However, in general the most significant impact from the L_u variation is obtained in the post stall mean wind region.
- The variation of A_{uu} (case 5) causes significant effects on all load categories, except the edge wise blade loading and the main shaft bending. A considerable dependence on the mean wind speed is seen.
- Neglecting the specified u-w and u-v turbulence cross-correlations (case 6) has significant fatigue load consequences in the post stall mean wind regime for all load categories, except for the edge wise blade loading and for the main shaft bending. In the linear and in the stall wind regime this parameter variation is without importance.

3.3 Vestas V39

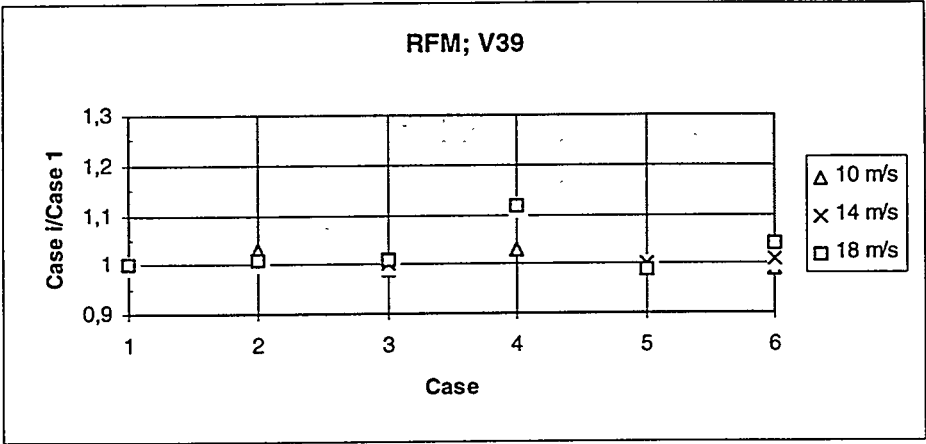


Figure 3.3-1 Relative importance of the selected parameter variations on RFM.

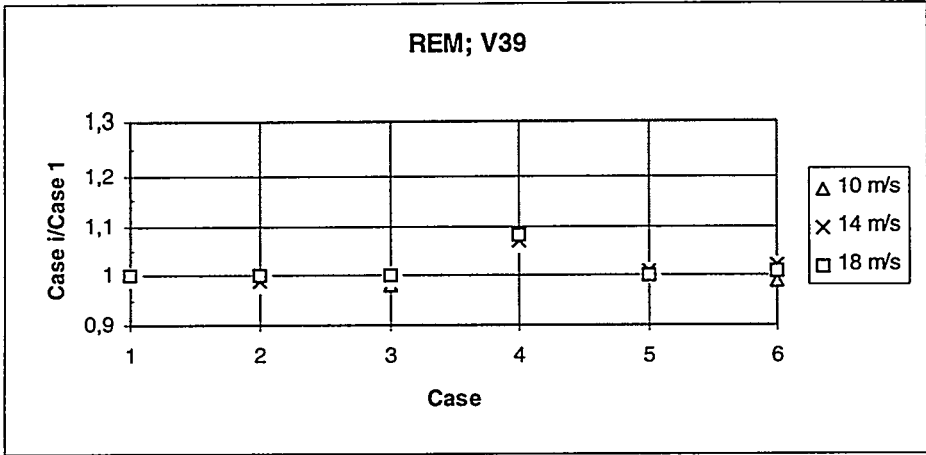


Figure 3.3-2 Relative importance of the selected parameter variations on REM.

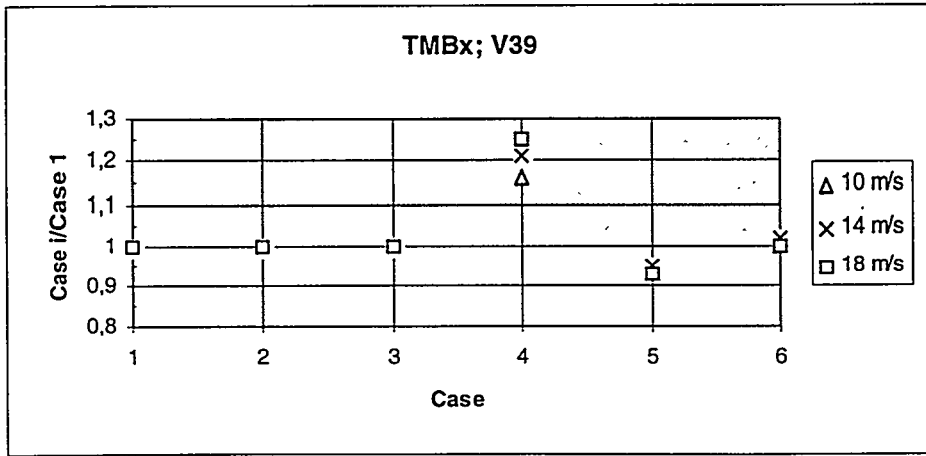


Figure 3.3-3 Relative importance of the selected parameter variations on TMBx.

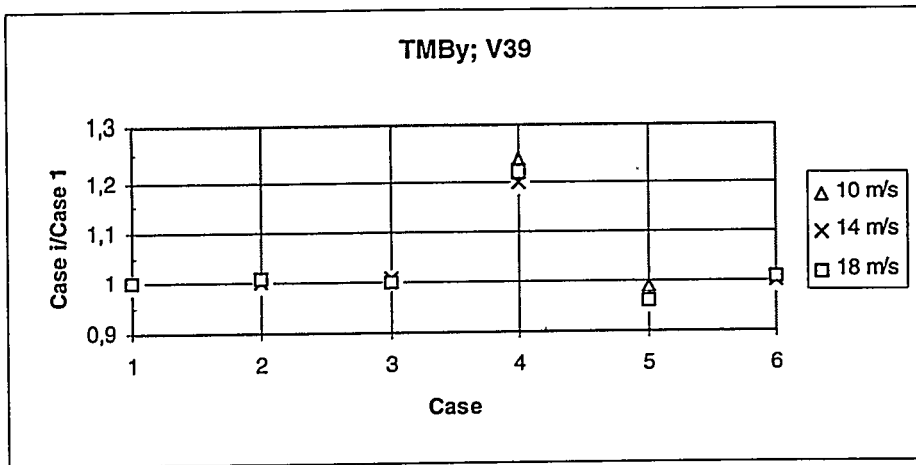


Figure 3.3-4 Relative importance of the selected parameter variations on TMBY.

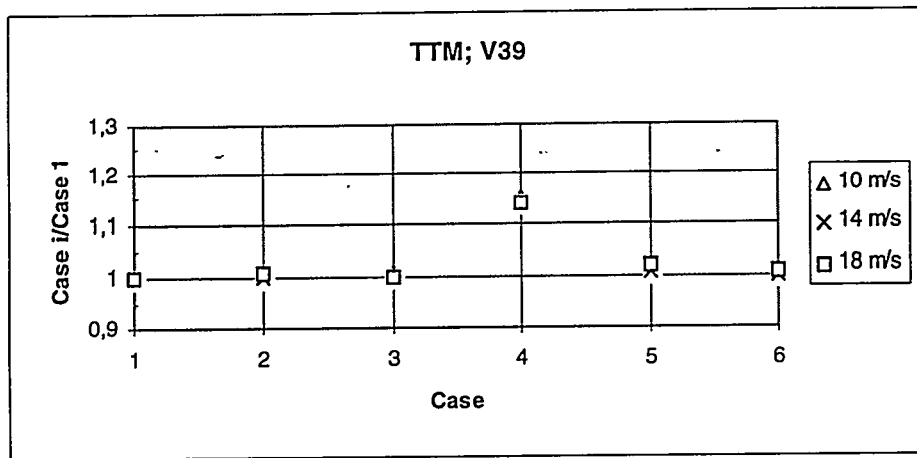


Figure 3.3-5 Relative importance of the selected parameter variations on TTM.

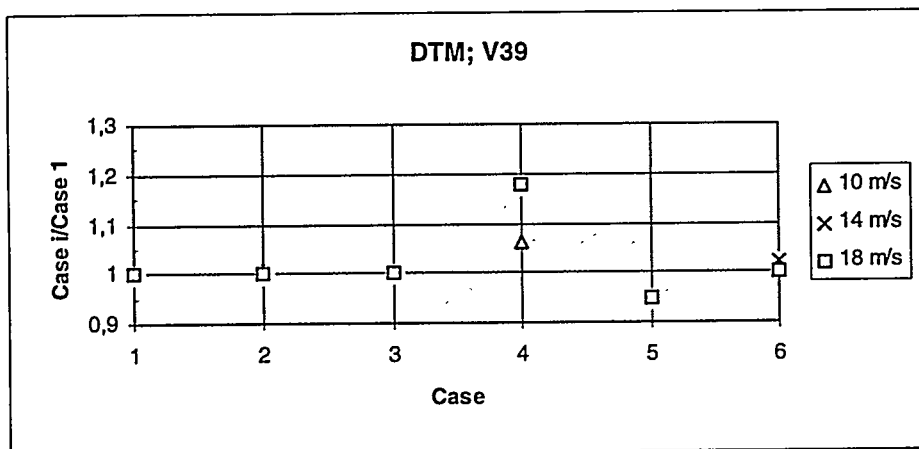


Figure 3.3-6 Relative importance of the selected parameter variations on DTM.

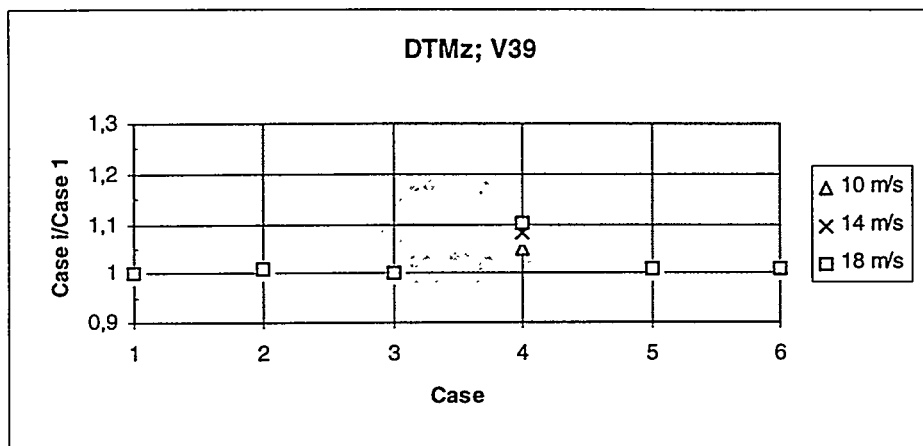


Figure 3.3-7 Relative importance of the selected parameter variations on DTMz.

Comparing Figures 3.1-1 to 3.1-7 and Figures 3.2-1 to 3.2-7 with the Figures 3.3-1 to 3.3-7, it is seen that the Vestas V39 wind turbine is the most robust of the investigated turbines concerning sensitivity to the performed parameter variations. The sensitivity of the Nordtank 500/37 turbine, equipped with a conventional tower, is, however, only marginally larger to the performed parameter variations than the Vestas V39 turbine.

The parameter variation, giving rise to the most significant modification in the fatigue loading on the Vestas V39 turbine, is the L_u variation (case 4), which affects all load categories including the edge wise blade loading. A considerable variation of the L_u sensitivity with the mean wind speed is observed for the flap wise-, the tower bottom bending- and for the drive train torque loading.

Besides the length scale variation, only the variation of the coherence decay factor A_{uu} (case 5) affects the fatigue loading significantly. However, the coherence decay variation do not affect all load categories, but primarily the tower bottom equivalent moment (TBMx) and the drive train (low speed) shaft equivalent moment (DTM).

In order to elucidate the individual differences between the considered three turbine concepts, the data material is reorganised in the Appendix A, such that a particular parameter effect, for a given load category and a given mean wind speed, is presented for all three turbines in the same plot.

4 Conclusion

Based on the analysis presented in Chapter 3, it can be concluded that the prescribed variation of the turbulence length scale in the mean wind direction gives rise to significant modification of the fatigue loading for all the three investigated wind turbine concepts.

The Vestas V39 wind turbine is the most robust of the investigated turbines, concerning sensitivity to the performed parameter variations, as only the length scale variation and coherence decay variation affect the fatigue loading of that machine. The sensitivity of the Nordtank 500/37 turbine, equipped with the conventional tower, is, however, only marginally more pronounced, concerning the performed parameter variations, than the Vestas V39 turbine.

The fatigue loading of the Nordtank 500/37 turbine, equipped with the conventional (stiff) tower, is significantly affected by the length scale variation for all response categories except the edge wise blade bending. To a more moderate extend it is further affected by the variation of the transversal turbulence intensity (flap wise bending and tower bottom bending), and by the specified variation in the vertical turbulence intensity (tower torsion moment). The variation in the uu coherence decay factor influence the fatigue loading in the tower bottom. The inclusion of the specified $u-w$ and $u-v$ turbulence cross-correlations showed up to be without importance for the investigated fatigue loads.

The Nordtank 500/37 turbine, equipped with the soft tower, is by far the most sensitive of the investigated turbine concepts to the performed parameter variations. Except for the edge wise blade loading, and to a less extend the main shaft bending, all the investigated fatigue loads are significantly affected by all the parameter variations. Furthermore, some quantitative and qualitative variations with the mean wind speed are observed.

5 References

- Thirstrup Petersen, J. (1990). Kinematically Nonlinear Finite Element Model of a Horizontal Axis Wind Turbine. Part 1 and 2. Risø National Laboratory, Roskilde, Denmark.
- Carlén, I.. SOSIS - A Wind Generator for Aeroelastic Calculations. To be published.
- Larsen, G.C. and Vølund, P. (1998). Validation of an Aeroelastic Model of Vestas V39. Risø-R-1051(EN). Risø National Laboratory, Roskilde, Denmark.
- Larsen, G.C. (1998). Fatigue Aspects of Soft Wind Turbine Towers. Risø-R-1059(EN). Risø National Laboratory, Roskilde, Denmark.
- Vølund, P. and Petersen, S.M. (1997). Validation of Aeroelastic Model of Nordtank 500/37. Risø-R-1006(EN). Risø National Laboratory, Roskilde, Denmark.
- Morfiadakis, E., Mouzakis, F. and Delaportas, P. (1996). Mounturb - Parameter Identification of Fatigue Loading of a Wind Turbine Operating in Complex Terrain. Centre for Renewable Energy Sources, C.R.E.S., Greece.
- Founda, D., Glinou, G., Kotronaros, A., Petrakis, M., Asimakopoulos, D. and Antoniou, I. (1993). Turbulence Characteristics of Relevance to Wind Turbines in Complex Terrain. EWEC'93, Travemünde, Germany.
- Teunissen, H.W. (1980). Structure of Mean Winds and Turbulence in the Planetary Boundary Layer over Rural Terrain. Boundary Layer Meteorology, 19, 187-221.

Appendix A

In order to elucidate the individual differences between the considered turbine concepts, the data material is reorganised in the present Appendix, such that a particular parameter effect, for a given load category and a given mean wind speed, is presented for all three turbines at the same plot.

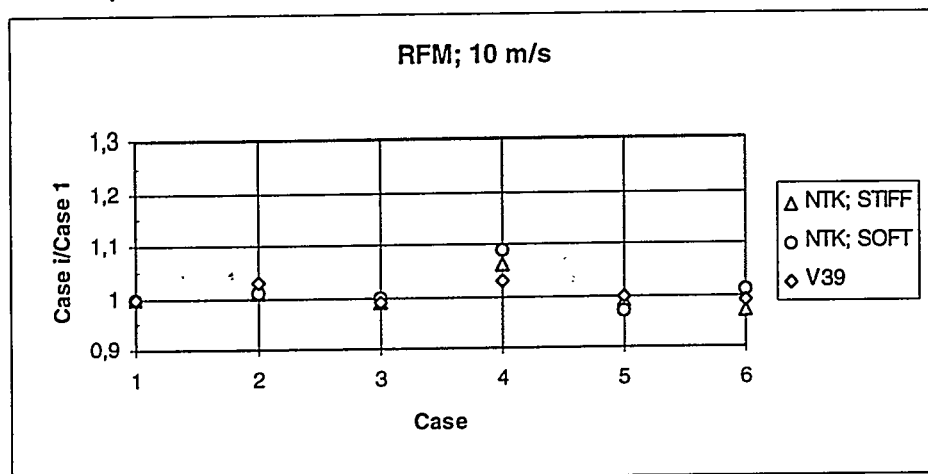


Figure A-1 Relative importance of the selected parameter variations on RFM (10 m/s).

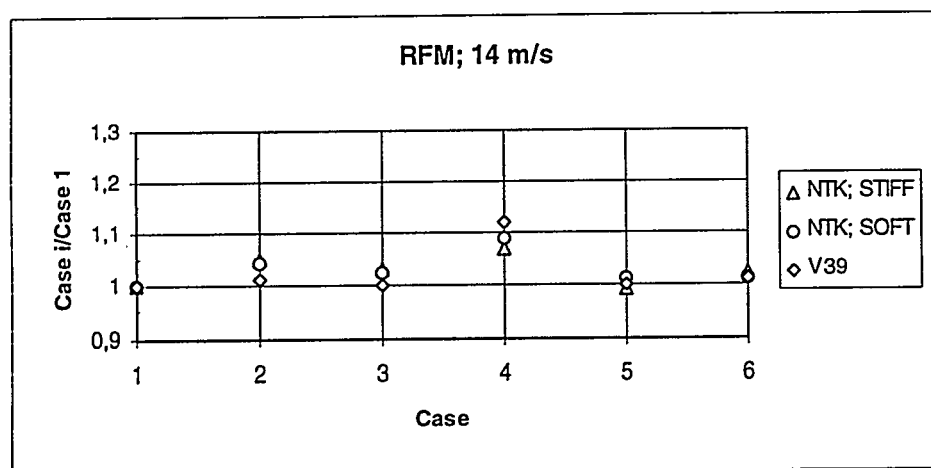


Figure A-2 Relative importance of the selected parameter variations on RFM (14 m/s).

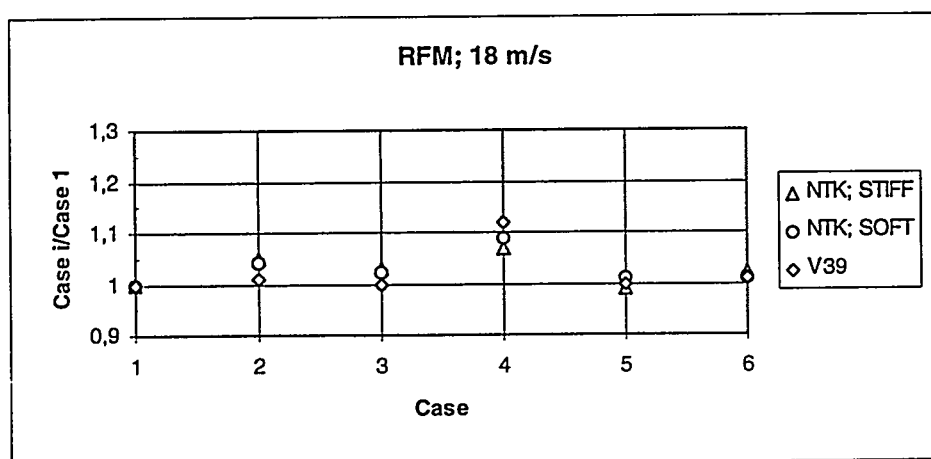


Figure A-3 Relative importance of the selected parameter variations on RFM (18m/s).

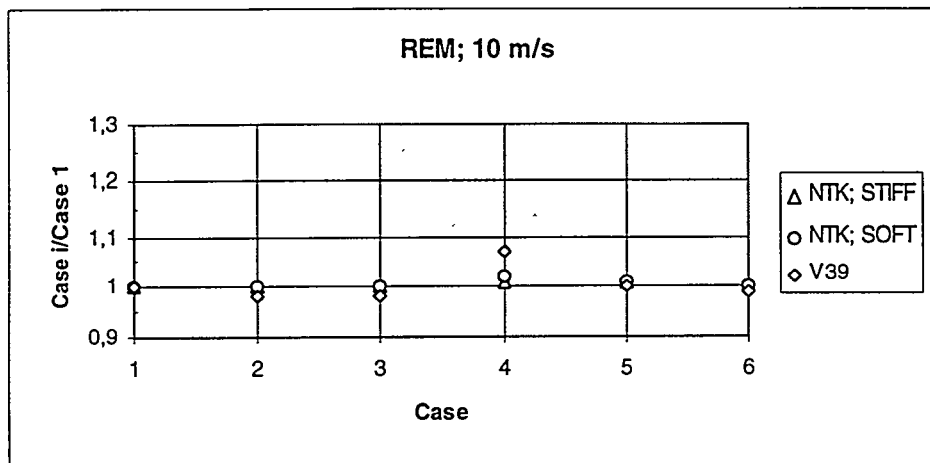


Figure A-4 Relative importance of the selected parameter variations on REM (10 m/s).

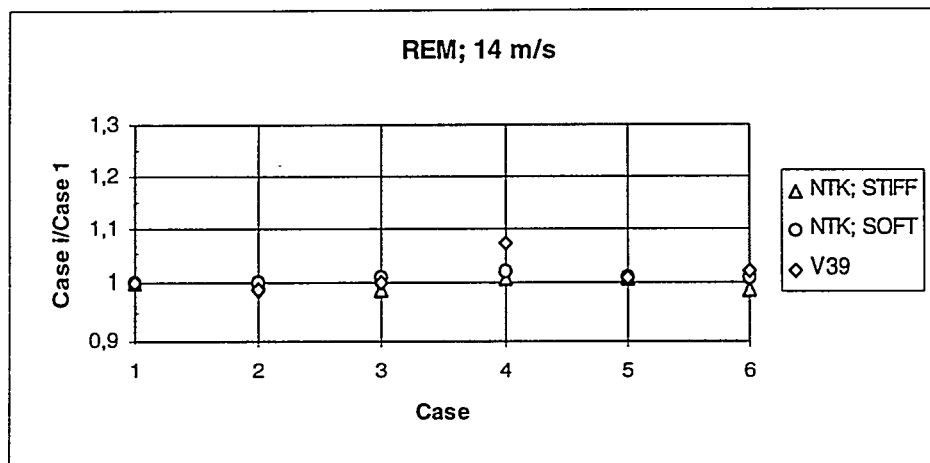


Figure A-5 Relative importance of the selected parameter variations on REM (14 m/s).

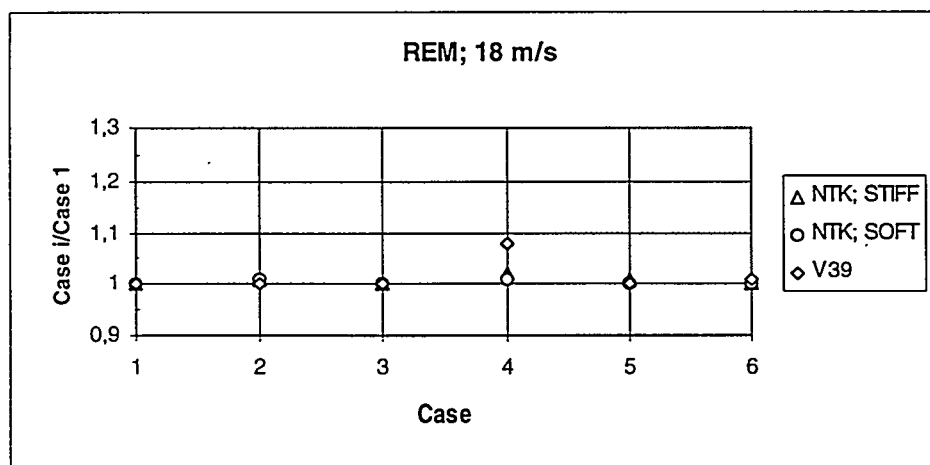


Figure A-6 Relative importance of the selected parameter variations on REM (18 m/s).

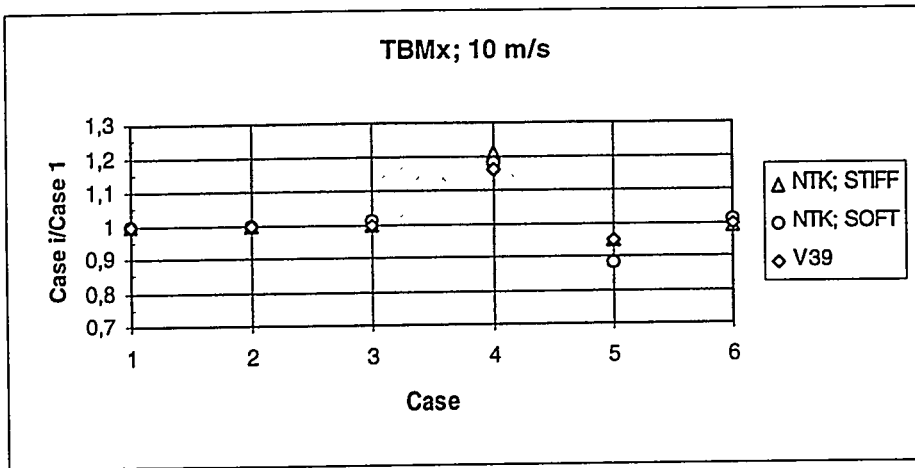


Figure A-7 Relative importance of the selected parameter variations on TBMx (10m/s).

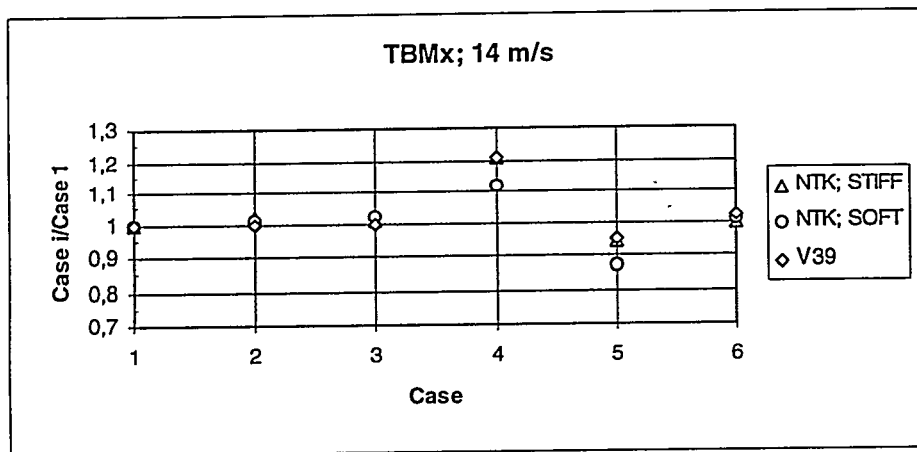


Figure A-8 Relative importance of the selected parameter variations on TBMx (14m/s).

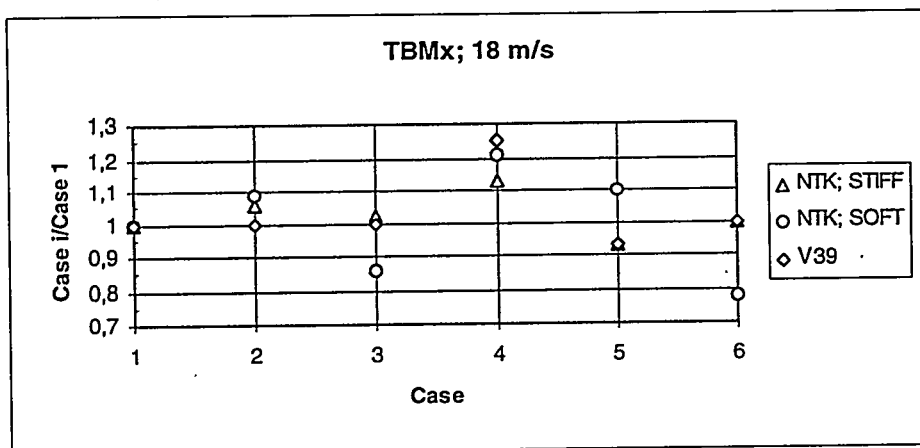


Figure A-9 Relative importance of the selected parameter variations on TBMx (18m/s).

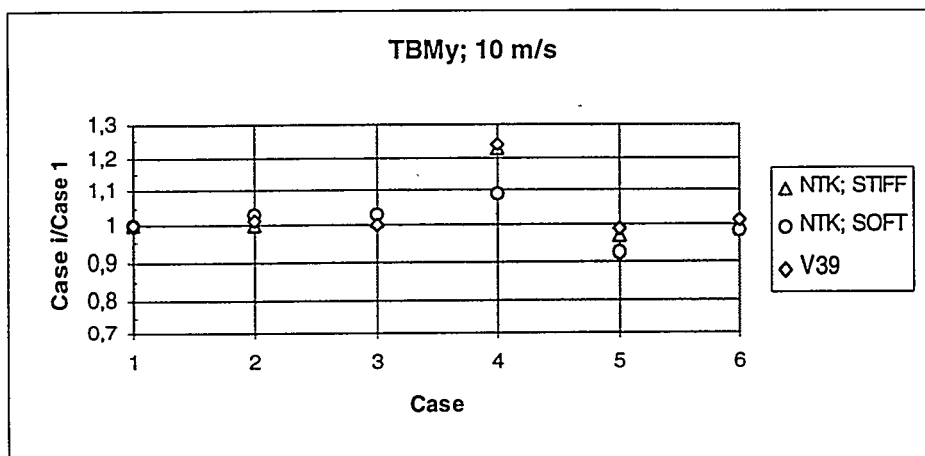


Figure A-10 Relative importance of the selected parameter variations on TBMy (10m/s).

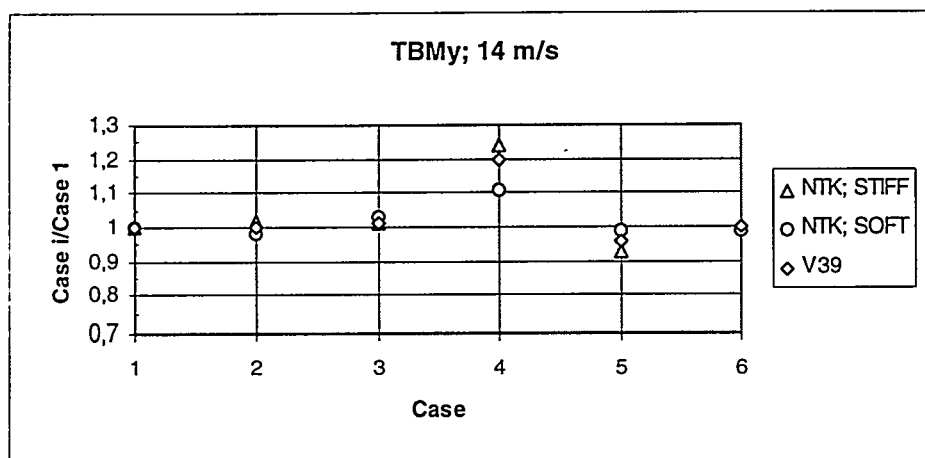


Figure A-11 Relative importance of the selected parameter variations on TBMy (14m/s).

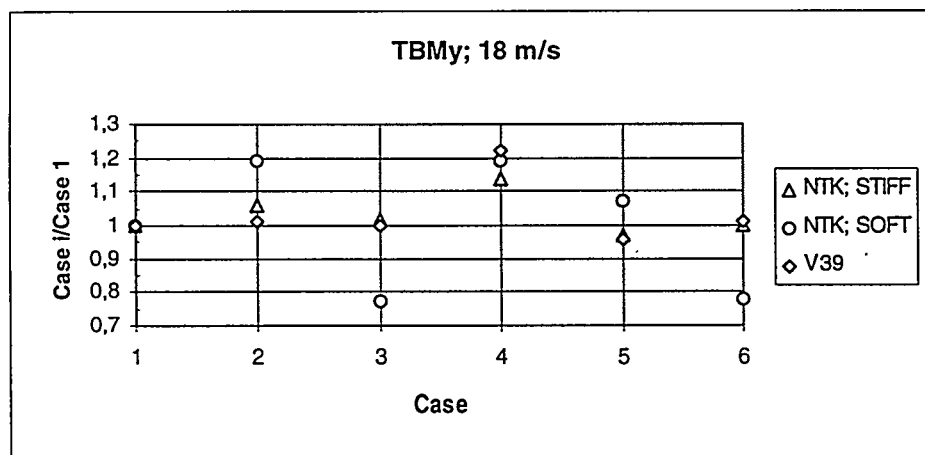


Figure A-12 Relative importance of the selected parameter variations on TBMy (18m/s).

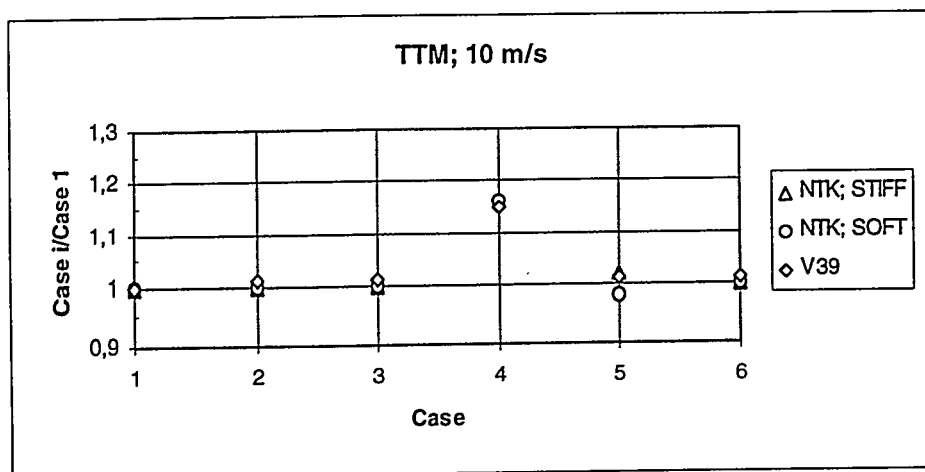


Figure A-13 Relative importance of the selected parameter variations on TTM (10m/s).

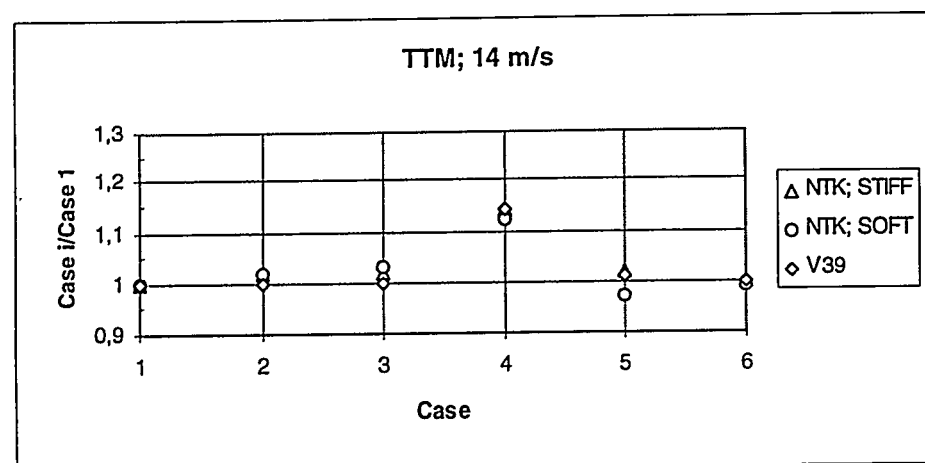


Figure A-14 Relative importance of the selected parameter variations on TTM (14m/s).

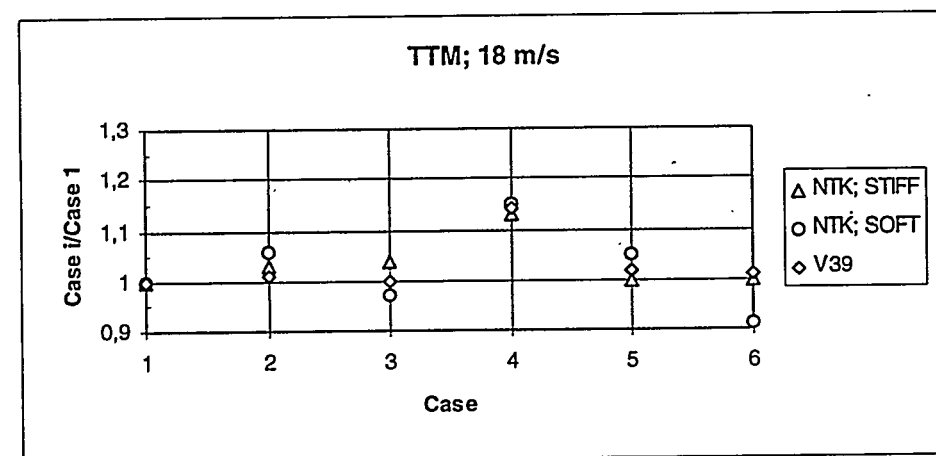


Figure A-15 Relative importance of the selected parameter variations on TTM (18m/s).

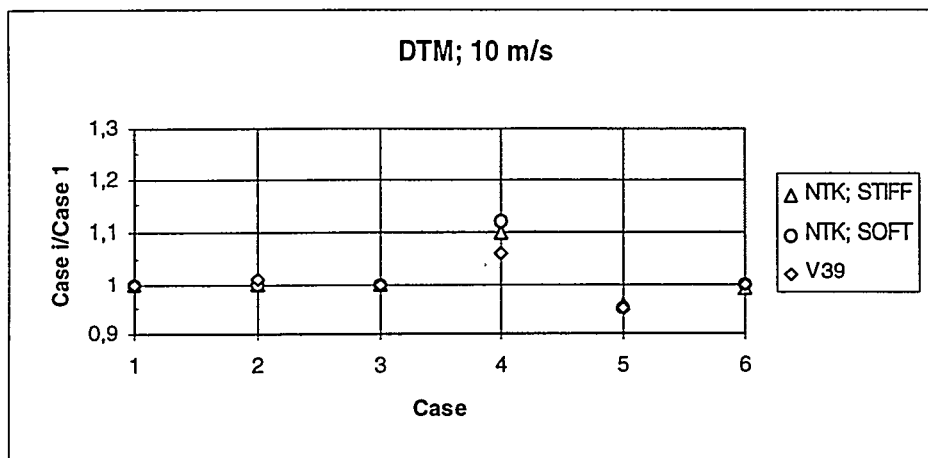


Figure A-16 Relative importance of the selected parameter variations on DTM (10m/s).

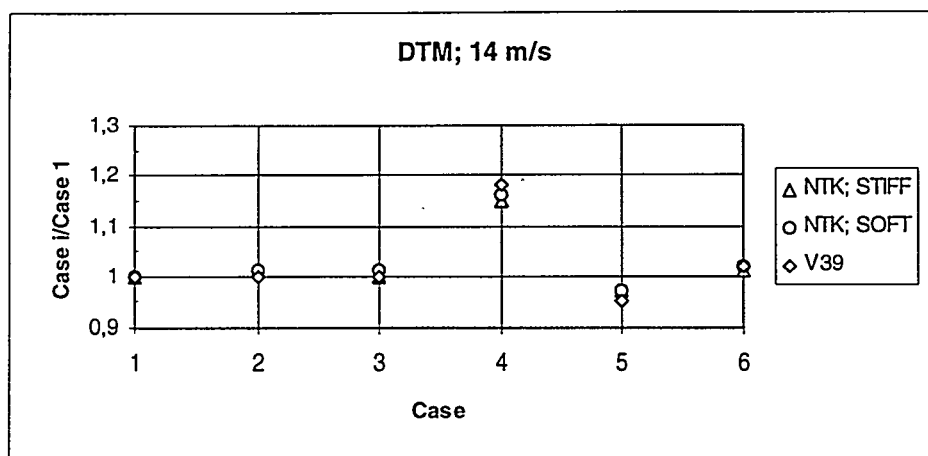


Figure A-17 Relative importance of the selected parameter variations on DTM (14m/s).

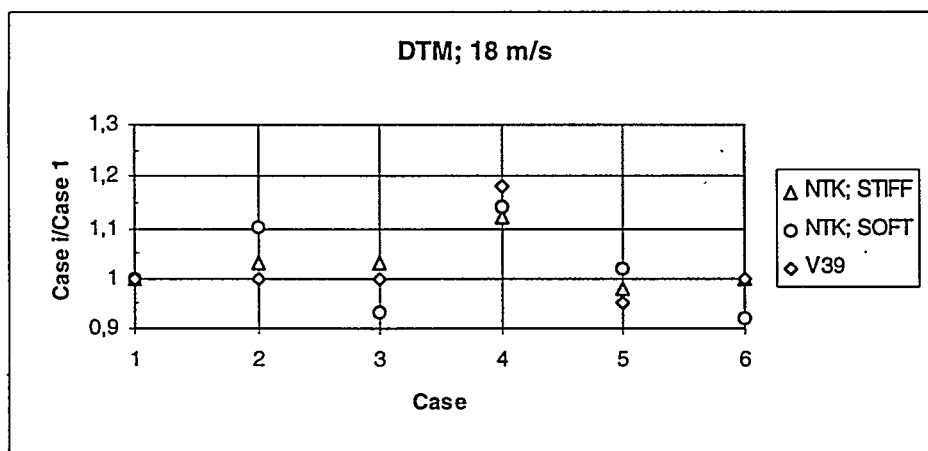


Figure A-18 Relative importance of the selected parameter variations on DTM (18m/s).

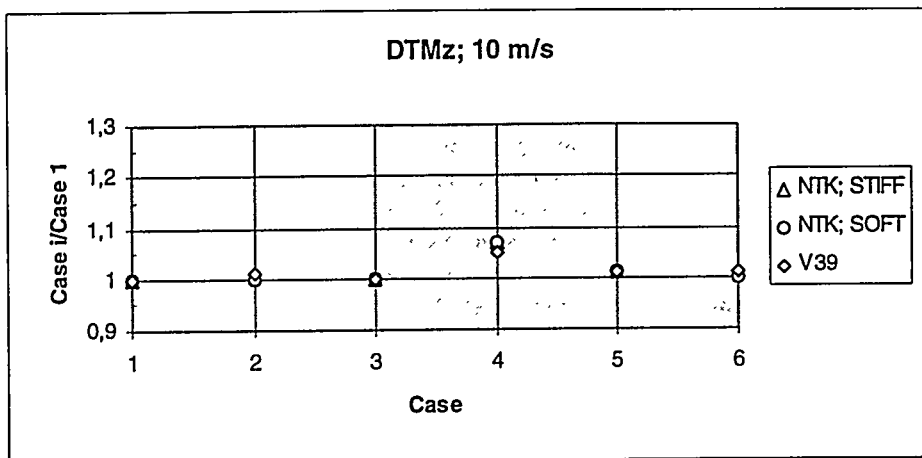


Figure A-19 Relative importance of the selected parameter variations on DTMz (10m/s).

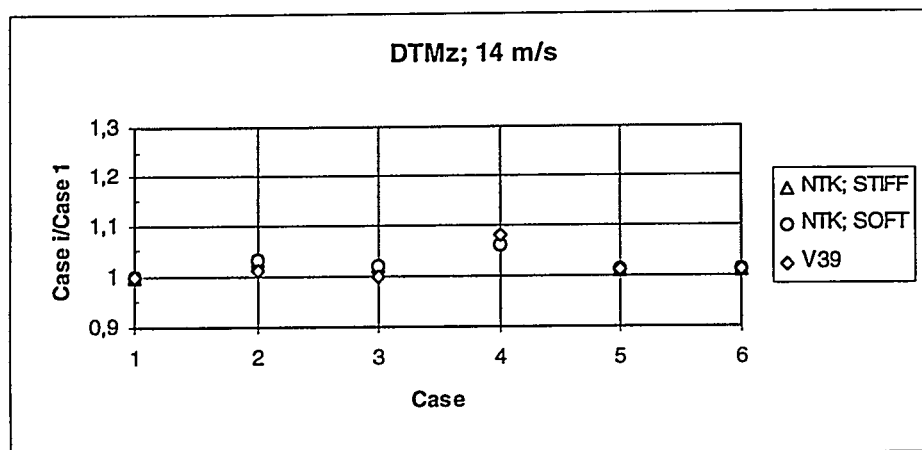


Figure A-20 Relative importance of the selected parameter variations on DTMz (14m/s).

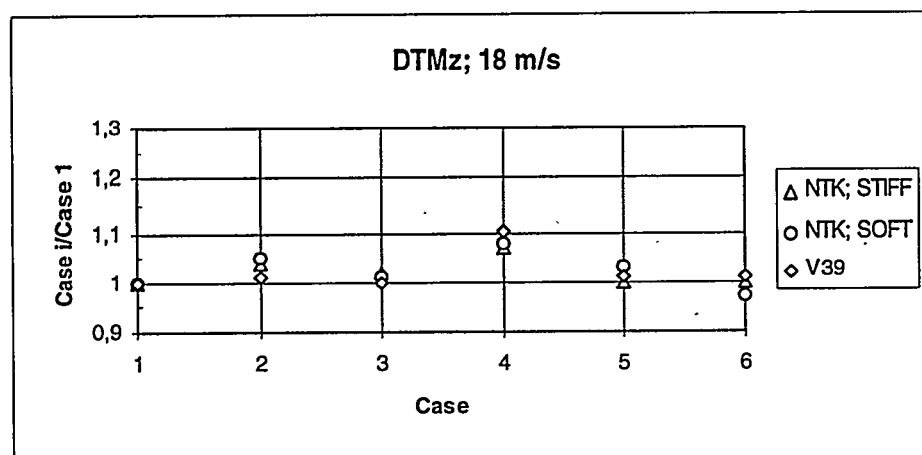


Figure A-21 Relative importance of the selected parameter variations on DTMz (18m/s).

Appendix B

The turbulence description in complex terrain, with highly varying topography and roughness, has been investigated in (Founda, 1993). Based on a large amount of data from the Kalivari hill at Andros in Greece, covering a broad variety of mean wind speeds and turbulence intensities, it was found that the Teunissen formulation (Teunissen, 1980) of the generic von Karman spectrum gave a better fit to the measured data than the generic Kaimal spectrum. Consequently, the von Karman spectrum has been applied in the present investigations of turbulence structure in complex terrain.

With conventional nomenclature, the u-, v- and w spectra are thus determined by:

$$\frac{\omega S_{uu}(\omega)}{\sigma_u^2} = \frac{4n_u}{(1 + 70.8n_u^2)^{5/6}} ; n_u = \frac{\omega L_u}{U},$$

$$\frac{\omega S_{vv}(\omega)}{\sigma_v^2} = \frac{4n_v(1 + 755.2n_v^2)}{(1 + 283.2n_v^2)^{11/6}} ; n_v = \frac{\omega L_v}{U},$$

$$\frac{\omega S_{ww}(\omega)}{\sigma_w^2} = \frac{4n_w(1 + 755.2n_w^2)}{(1 + 283.2n_w^2)^{11/6}} ; n_w = \frac{\omega L_w}{U},$$

where L denotes the turbulence length scale and U is the mean wind velocity.

Title and authors

Consequences of Variations in Spatial Turbulence Characteristics for Fatigue Life Time of Wind turbines

Gunner Chr. Larsen

ISBN

87-550-2432-7

87-550-2433-5 (Internet)

ISSN

0106-2847

Department or group

Wind Energy and Atmospheric Physics Department

Date

September 1998

Groups own reg. number(s)

1120058-00

Project/contract No(s)

JOR3-CT95-0033

Pages

29

Tables

2

Illustrations

43

References

7

Abstract (max. 2000 characters)

The fatigue loading of turbines situated in complex terrain is investigated in order to determine the crucial parameters in the spatial structure of the turbulence in such situations. The parameter study is performed by means of numerical calculations, and it embraces three different wind turbine types, representing a pitch controlled concept, a stall controlled concept, and a stall controlled concept with an extremely flexible tower.

For each of the turbine concepts, the fatigue load sensibility to the selected turbulence characteristics are investigated for three different mean wind speeds at hub height. The selected mean wind speeds represent the linear-, the stall-, and the post stall aerodynamic region for the stall controlled turbines and analogously the unregulated-, the partly regulated-, and the fully regulated regime for the pitch controlled turbine. Denoting the turbulence component in the mean wind direction by u , the lateral turbulence component by v , and the vertical turbulence component by w , the selected turbulence characteristics comprise the u -turbulence length scale, the ratio between the v - and w -turbulence intensities and the u -turbulence intensity, the uu -coherence decay factor, and finally the u - v and u - w cross-correlations.

The turbulence length scale in the mean wind direction gives rise to significant modification of the fatigue loading on all the investigated wind turbine concepts, but for the other selected parameter variations, large individual differences exists between the turbines. With respect to sensitivity to the performed parameter variations, the Vestas V39 wind turbine is the most robust of the investigated turbines. The Nordtank 500/37 turbine, equipped with the (artificial) soft tower, is by far the most sensitive of the investigated turbine concepts - also much more sensitive than the conventional Nordtank 500/37 turbine equipped with a traditional tower.

Descriptors INIS/EDB

COMPLEX TERRAIN; COMPUTERIZED SIMULATION; ELASTICITY; FATIGUE; HORIZONTAL AXIS TURBINES; SERVICE LIFE; TURBULENCE; WIND LOADS.

Available on request from Information Service Department, Risø National Laboratory,

(Afdelingen for Informationsservice, Forskningscenter Risø), P.O.Box 49, DK-4000 Roskilde, Denmark.

Telephone +45 46 77 40 04, Telefax +45 46 77 40 13